A&A 467, 259–268 (2007)
DOI: 10.1051/0004-6361:20066991

Astronomy & Astrophysics

The narrowest M-dwarf line profiles and the rotation-activity connection at very slow rotation⋆

A. Reiners[1,2,⋆⋆]

[1] Universität Göttingen, Institut für Astrophysik, Friedrich-Hund-Platz 1, 37077 Göttingen, Germany
e-mail: Ansgar.Reiners@phys.uni-goettingen.de
[2] Universität Hamburg, Hamburger Sternwarte, Gojenbergsweg 112, 21029 Hamburg, Germany

Received 20 December 2006 / Accepted 21 February 2007

ABSTRACT

Context. The rotation-activity connection explains stellar activity in terms of rotation and convective overturn time. It is well established in stars of spectral types F–K as well as in M-type stars of young clusters, in which rotation is still very rapid even among M-dwarfs. The rotation-activity connection is not established in field M-dwarfs, because they rotate very slowly, and detecting rotation periods or rotational line broadening is a challenge. In field M-dwarfs, saturation sets in below $v_{\rm rot} = 5\,{\rm km\,s^{-1}}$, hence they are expected to populate the non-saturated part of the rotation-activity connection.
Aims. This work for the first time shows intrinsically resolved spectral lines of slowly rotating M-dwarfs and makes a first comparison to estimates of convective velocities. By measuring rotation velocities in a sample of mostly inactive M-dwarfs, the unsaturated part of the rotation-activity connection is followed into the regime of very low activity.
Methods. Spectra of ten M-dwarfs are taken at a resolving power of $R = 200\,000$ at the CES in the near infrared region where molecular FeH has strong absorption bands. The intrinsically very narrow lines are compared to model calculations of convective flows, and rotational broadening is measured.
Results. In one star, an upper limit of $v \sin i = 1\,{\rm km\,s^{-1}}$ was found, significant rotation was detected in the other nine objects. All inactive stars show rotation below or equal to $2\,{\rm km\,s^{-1}}$. In the two active stars AD Leo and YZ CMi, rotation velocities are found to be 40–50% below the results from earlier studies.
Conclusions. The rotation activity connection holds in field early-M stars, too. Activity and rotation velocities of the sample stars are well in agreement with the relation found in earlier and younger stars. The intrinsic absorption profiles of molecular FeH lines are consistent with calculations from atomic Fe lines. Investigation of FeH line profiles is a very promising tool to measure convection patterns at the surfaces of M-stars.

Key words. stars: late-type – stars: activity – stars: rotation

1. Introduction

The connection between rotation and activity among sun-like stars allows a look inside the nature of the magnetic dynamo hosted in sun-like stars. The rotation-activity connection is established in late-type stars (mid F – early M) through all ages and spectral types for which rotation can be measured (e.g., Noyes et al. 1984; Patten & Simon 1996). It is believed that a rotation-dependent dynamo process generates large-scale magnetic fields that heat the upper layers of the atmosphere and cause the variety of activity phenomena observed in the Sun and other stars. Tracers of stellar activity are X-ray emission and chromospheric emission lines like Hα and Ca H & K. For a given spectral type, the strength of activity depends on rotation in the sense that among slow rotators (here, the definition of "slow" depends on spectral type, see below) activity grows with rotation speed, but at a certain angular velocity, activity becomes saturated and does not grow with more rapid rotation.

Between different spectral types, the dependence of activity on stellar rotation rate is slightly different. This is believed to be due to the different efficiencies of the stellar dynamo, which depends on the dynamo number $N_{\rm D}$ (Parker 1971), but there is also some debate whether this dependence is only seen when normalizing emission measures to bolometric luminosity (Basri 1986; Pizzolato et al. 2003). Durney & Latour (1978) suggested a relationship between dynamo number $N_{\rm D}$ and Rossby number Ro of the form $N_{\rm D} \approx Ro^{-2}$ (see also Noyes et al. 1984), while $Ro \propto P/\tau_{\rm conv}$, with P the rotation period and $\tau_{\rm conv}$ the convective overturn time, the latter is the factor that depends on spectral type. The criterion for a dynamo to work is $N_{\rm D} \gtrsim 1$ ($Ro \lesssim 1$), i.e., rotation is stronger than convection. Noyes et al. (1984) showed that plotting the chromospheric emission ratio $R'_{\rm HK}$ vs. Rossby number significantly reduces the scatter that appears when plotting $R'_{\rm HK}$ vs. rotation period. Patten & Simon (1996); Randich et al. (1996) and Pizzolato et al. (2003) used this to show that the rotation-activity connection is universal in cluster and field stars of different age and spectral type.

1.1. Rotation and activity in early M-stars

Stars of spectral type M are places of frequent flaring events. These stars have relatively low temperatures while flaring activity stems from high temperature plasma, thus their UV and optical colors are subject to enormous brightness variations. Activity

⋆ Based on observations carried out at the European Southern Observatory, La Silla, PID 076.D-0092.
⋆⋆ Marie Curie Outgoing International Fellow.

in field M-stars was observed in X-rays (e.g., Barbera et al. 1993; Fleming et al. 1993; Schmitt et al. 1995; Giampapa et al. 1996) and Hα (e.g., Herbst & Miller 1989; Hawley et al. 1996; Delfosse et al. 1998; Gizis et al 2002; Mohanty & Basri 2003; West et al. 2004). The Ca H & K lines are difficult to measure since they have very little flux in the M-stars. All measurements led to the picture that M-stars can be very active, and West et al. (2004) shows that the fraction of active M-stars is rather low at early subclasses but rises dramatically around spectral type M4, up to ∼75% at M7 before it goes down again at the late M-type objects. The falloff towards spectral class L is explained by the high electrical resistivity in such cool atmospheres (Fleming et al. 2000; Mohanty et al. 2002).

The validity of the rotation-activity connection was shown in a large range of stars of different age and spectral type. Measurements of activity are available for a huge number of targets provided by a wealth of different instruments either spectroscopically, from dedicated imaging projects or large sky surveys. Measuring rotation, however, requires either to follow brightness variations over some time to observe periodic changes due to presumably corotating features on the stellar surface, or the analysis of a high-quality spectrum to detect rotational line broadening in spectral features.

The saturated part of the rotation-activity connection, i.e. fast rotators, is well established since short periods as well as strong rotation broadening are relatively easy to measure. The non-saturated part of this connection, however, consists of the slower rotators with longer rotation periods and weaker rotational line broadening. This poses a big problem to the measurement of the rotation-activity connection in M-stars, where convective overturn times are longest leading to rotation periods of several weeks and – due to the small radii – to very small surface velocities.

The measurement of rotation periods in M-stars is particularly difficult since on active stars flares occur on timescales much shorter than the rotation period which effectively hides the rotation period under the noise of stellar activity. The measurement of a long period requires extremely high data quality and time coverage (e.g. Benedict et al. 1998). If, on the other hand, a star is inactive, there is little rotational variation in its lightcurve so that the detection of a period is difficult or impossible. Detections of rotation periods in M-stars are still very limited; Pettersen (1982) reports rotation periods in 11 Me-dwarfs in the range 1–8 d, all of them translate into surface velocities larger than 4 km s^{-1}. Torres et al. (1982) report three significant detections of rotation periods, again in dMe stars. The amount of questionable results (indicated with questionmarks in their Table II) and the paucity of later successful detections of M-star rotation periods demonstrate the difficulty detecting them[1].

To follow the rotation activity connection to the slowest rotators in old (hence slowly rotating) M-stars, the measurement of the rotation velocity is often the easier way. How does the rotation activity relation look if one uses $v \sin i$ instead of rotation period or Rossby number? In Fig. 1, the mean rotation activity connection from Patten & Simon (1996) is shown as an activity vs. equatorial velocity plot. Due to different radii and convective turnover times, the one relation found for spectral types mid-F to early-M spreads in spectral type. In the low-mass stars, the rising part is shifted to smaller velocities. This is shown for four different spectral types, G1, G8, K2, and M2 in Fig. 1. While stars of spectral type G1 are saturated at a velocity of almost 30 km s^{-1}, M2-stars are already saturated at about 5 km s^{-1}. Note that the translation of the empirical relation also depends on the chosen value for the overturn time $\tau_{\rm conv}$, which is difficult to compute particularly in very cool stars. The semi-empirical values of Noyes et al. (1984) were chosen for Fig. 1. Gilliland (1986) and Kim & Demarque (1996) also calculated $\tau_{\rm conv}$ and gave somewhat higher $\tau_{\rm conv}$ for M-stars. This would translate into even smaller rotation velocities for the M2 example.

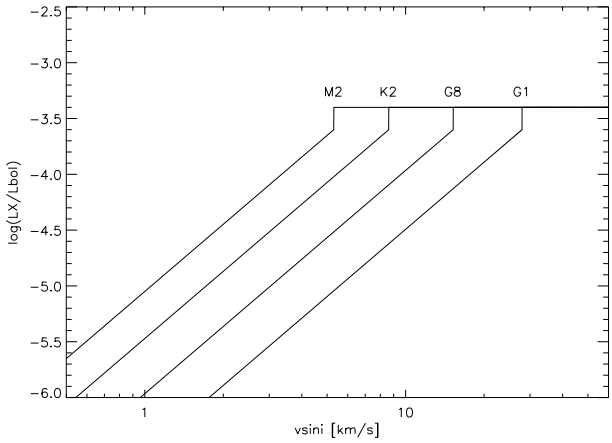

Fig. 1. Mean rotation activity connection from Patten & Simon (1996) with Rossby number translated into surface velocity shown for four spectral types. Due to different radii and convective turnover times, the relation spreads in spectral type, in the M-dwarfs the rising part falls below $v = 5$ km s^{-1}.

In Fig. 1, one can see that resolving the rotation activity connection among field M-dwarfs requires the measurement of rotational line broadening on the order of 1 km s^{-1}. Unfortunately, two mechanisms work against the observer; a) high spectral resolution requires a lot of photons, but the targets are very faint; b) detecting slow rotation requires sharp spectral features, but spectra of M-dwarfs are covered with molecular absorption bands eating away the continuum. Individual atomic lines as in the solar spectrum are hardly available at all since most lines are too weak at such low temperatures, and the strong alkali lines are so pressure broadened that the signature of slow rotation is washed out.

1.2. Measuring very slow rotation

The measurement of Doppler line broadening due to very slow rotation requires high spectral resolution so that it is not dominated by instrument effects. In principle, one can correct for instrumental broadening if accurately known. In the presence of noise and blended spectral lines, however, rotational broadening is only detectable if it is on the order of the instrument profile. In other words, slow rotation on the order of 1 km s^{-1} has very little influence on a line profile observed at a limited resolution of, e.g., 5 km s^{-1}, but it will be easily detectable if the instrumental profile is only 1 km s^{-1} wide. Furthermore, broadening effects other than rotation (convection, Zeeman splitting, etc.) may influence the line shape as well. The line profile of a "non-rotating" M-star has a *FWHM* on the order of 6–7 km s^{-1} at a resolution of $R \sim 50\,000$ and on the order of 2 km s^{-1} at a resolution of $R \sim 200\,000$. With the lower resolution, such a profile is sampled in only 1–2 resolution elements while at high resolution it

[1] Note that Spiesman & Hawley (1986) claim the detection of a rotation period in AD Leo that is comparable to the one of Torres et al. (1982) (indicated as questionable in their work). The fact that both groups find the same period may suggest that AD Leo indeed rotates at $P \approx 2.7$ d. However, the detection remains somewhat tentative in both works.

Table 1. Sample stars, observations and targets used for flatfielding.

Name	Sp type[a]	m_I[b]	Exp. time [min]	*SNR*[c]
Gl 514	M0.5	7.04	65	45
Gl 229A	M1.0	6.11	60	80
Gl 526	M1.5	6.43	45	45
Gl 205	M1.5	5.88	50	85
Gl 382	M1.5	7.09	85	50
Gl 393	M2.0	7.41	60	45
Gl 273	M3.5	7.16	110	50
Gl 388/AD Leo	M3.5	6.81	60	40
Gl 628	M3.5	7.40	30	30
Gl 285/YZ CMi	M4.5	8.20	90	20
Telluric Standards used as Flatfields				
HD 74956	A1V	1.86	10	
HD 47670	B8III	3.24	30	

[a] Reid et al. (1995); Hawley et al. (1996). [b] Leggett (1992). [c] Per pixel, *SNR* per resolution element is about a factor of two higher.

is seen in about 5–10 resolution elements. Clearly, projected rotation velocities of $v \sin i \approx 2\,\mathrm{km\,s^{-1}}$ are difficult to detect in the former case but easily detectable in the latter.

Another technique that is frequently used to determine rotation in M-dwarfs is the cross-correlation technique. The width of the cross-correlation profile between a slowly rotating template and the target star is used as an indicator for rotation velocity. This strategy partly overcomes the problem of low signal-to-noise ratio (*SNR*) and the lack of isolated spectral features since it utilizes larger wavelength regions that show characteristic features. Molecular bands have been used even in late M- and L-dwarfs (Mohanty & Basri 2003; Bailer-Jones 2004). However, one cannot expect the method to yield lower detection thresholds at very low rotation since the width of the cross-correlation profile cannot be more sensitive to small rotation than the direct comparison of narrow lines is (note that the cross-correlation profile is generally broader than the narrowest lines, this weakens the advantage of the higher *SNR* of the cross-correlation profile at slow rotation). Furthermore, even small template mismatch and other systematic uncertainties (e.g., uncertainties in the continuum normalization) always lead to a *wider* cross-correlation profile, i.e. too high a rotation velocity – no effect can lead to a cross-correlation profile that is narrower than the one for the correct rotation broadening.

In this paper, I present the first spectra of absorption lines that resolve intrinsic line broadening in M stars, i.e. isolated absorption lines not dominated by the instrumental profile or rotation. Molecular absorption of FeH around 1 μm are intrinsically narrow and well isolated so that they provide an ideal tracer of M-dwarf line broadening due to convection or very slow rotation ($v \sin i < 3\,\mathrm{km\,s^{-1}}$, Reiners & Basri 2006). At a resolving power of $R \sim 200\,000$, these data carry information on slow rotation and surface velocity patters that are not contained in data of lower spectral resolution. The data will be described in more detail in Sect. 2. Rotation velocities are measured and put into context with activity measurements in Sects. 3 and 4. A summary is provided in Sect. 5.

2. Data

Data were taken at the Coudé Echelle Spectrograph (CES) at the 3.6 m telescope, ESO, La Silla. The spectral region at 1 μm is exceptionally red for its front-illuminated CCD resulting in relatively poor efficiency and heavy fringing. However, since the spectral region is near the peak of the spectral energy distribution of M-stars, high *SNR* could be achieved with relatively short exposures. Exposure times and *SNR* are given in Table 1 together with the apparent I-magnitudes from Leggett (1992). The high resolution of $R \sim 200\,000$ is achieved through an image slicer chopping the light from the star in 12 narrow slices. The instrument is fibre-fed and no geometric information is conserved after the light has passed through fibre and slicer. Unfortunately, this means that the fringing pattern of the CCD depends on how the fibre is illuminated. As a consequence, the fringing in the on-star observations cannot be corrected for using a flatfield exposure that uniformly illuminates the fibre instead of providing a point source as the stars do. Thus, the flatfields taken at the CES are useless in this spectral region. In order to correct for the heavy fringing, high-*SNR* exposures of two telluric standard stars were taken, and they were used as 2D flatfields during the reduction procedure. Observations of both flatfields were combined to yield highest *SNR*[2].

Using telluric reference stars to correct for the pixel to pixel sensitivity also eliminates telluric features if observations of the target stars are taken at very similar airmass. As shown in Reiners & Basri (2006), the spectral region near 1 μm is virtually free of telluric contamination so that no telluric correction seems necessary. Thus, standard stars were taken at arbitrary position (furthermore, no stars bright enough for this project are available next to each target).

The sample consists of the brightest slowly rotating M-dwarfs visible in early spring at La Silla, Chile. Several inactive stars with rotation velocities too low for previous measurements were chosen in order to resolve slow rotation in the unsaturated part of the rotation-activity connection at spectral types where stars become fully convective. Three stars with detected rotation were observed as well, two of them (AD Leo and YZ Cmi) very active stars with saturated coronal emission.

3. Rotation analysis

In this paper, rotation is measured comparing the shape between lines of the slowest rotator (the template) and the other targets. Rotation velocities are found by artificially broadening the narrow lines of the template star. To do so, it is essential to find isolated and intrinsically narrow spectral lines that are embedded in a clear continuum. In the classical optical wavelength regions, such lines are difficult to find since TiO and VO have strong absorption systems in this region. However, at longer wavelengths around 1 μm, the main opacity sources TiO and VO do not show absorption bands, and the only features are lines of molecular FeH. This absorption band was investigated by Reiners & Basri (2006), it consists of many isolated lines of FeH, many clearly discernible and intrinsically narrow. The lines are embedded in a clear continuum which allows to accurately follow individual line profiles from the core to the wings. Among the M dwarfs, the structure of the FeH band follows an optical depth scaling so that FeH lines of any M dwarf spectrum can be reproduced by scaling the FeH band of a template star that may have a different spectral class (Reiners & Basri 2006). A part of the CES spectrum in the FeH region is shown in Fig. 2. The two lines, λ9941.9 and λ9950.4 Å, that are used to determine rotational broadening are indicated in the figure.

[2] Flatfielding was done in the 2D-images. The reduced flatfield spectrum would have a *SNR* of ~300.

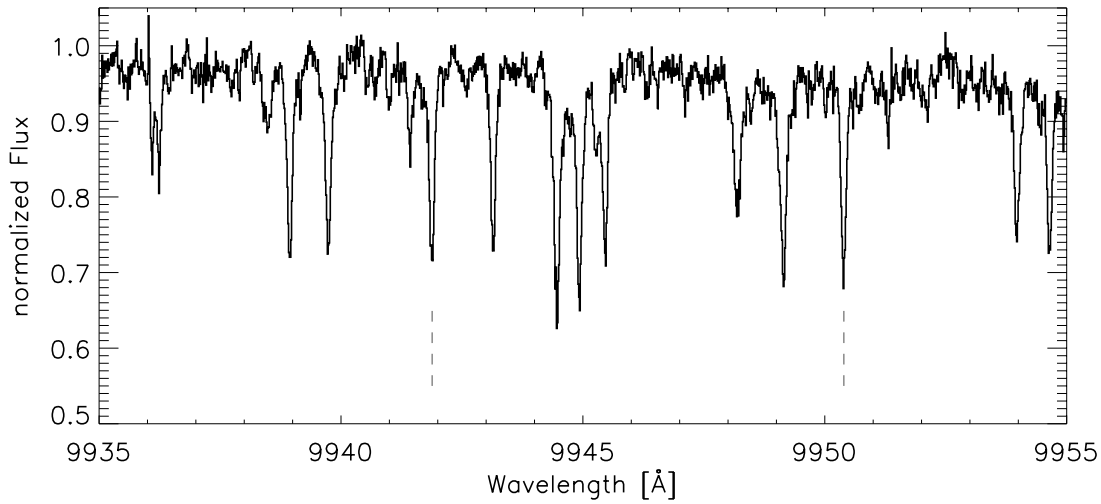

Fig. 2. Part of the spectrum of Gl 273 observed with the CES. The two magnetically insensitive lines at 9941.9 Å and 9950.4 Å that are used for rotation analysis are marked.

The most reliable way determining rotational line broadening is to utilize the spectrum of a star that shows virtually no rotation, i.e. $v \sin i$ is below the detection limit. The width of the narrowest line that can possibly be observed in a spectrum depends I) on the instrumental resolution, and II) on the intrinsic line width without rotation, i.e. effects like temperature broadening, pressure broadening, and convection. The star with the narrowest profile in the sample is Gl 273, which is also the star with the lowest ratio L_X/L_{bol}. No rotation has been detected in this star before and there is no reason to assume that significant broadening due to rotation affects its line profile. Nevertheless, the line profiles of the FeH lines in Gl 273 are well resolved and they are significantly broader than the instrumental profile as discussed in the following.

Recently, López-Morales (2007) has shown that a connection exists between radius and metallicity in single M dwarfs, and between radius and activity in very active members of binary systems. The stars in the sample analyzed here are single stars with relatively low activity, so that no effect regarding the radius of the stars is expected through strong activity. The radii of the stars may differ a little among the same spectral type due to metallicity effects. However, the FeH lines analyzed in this work are insensitive to gravity (and hence radius). No effects on the derivation of $v \sin i$ are expected.

3.1. The slowest rotator

The two spectral lines λ9941.9 and λ9950.4 Å of Gl 273 are shown in the left column of Fig. 3 in velocity units relative to the line center. Data are plotted with error bars according to the measured *SNR* given in Table 1. The instrumental profile measured from ThAr lines is overplotted (magenta), it is significantly smaller than the observed line showing that the line shape has been resolved. Unfortunately, radiative transfer calculations of the FeH lines are not yet available so that it was not possible to compare the line shape to a fully consistent model of the two molecular lines. However, the main broadening mechanisms in such narrow lines are temperature broadening and convective velocities. The atomic weight of Fe is a good approximation of the weight of the FeH molecule, thus temperature broadening in Fe lines can be expected to be very similar to the effect in FeH lines. The strength of the FeH lines in early M stars is also comparable to some Fe lines, so that the line formation depths should also be similar in both species. Thus, line broadening due to convective motions are probably of comparable strength.

In Fig. 3, a model of the intrinsic profile of the Fe I line at $\lambda = 6518.37$ Å for $T_{\rm eff} = 2800$ K and $\log g = 5.0$ is shown (cyan). The profile was kindly provided by Wedemeyer & Ludwig (priv. comm.). Atmospheric parameters correspond to an M6 atmosphere which is slightly cooler than our target objects. It is not the aim of this study to perform a detailed comparison to the model spectrum, which only serves as a consistency check for the observed line profile in the slowest rotator. The difference in temperature broadening between the model star and Gl 273 implies a difference between the observed lines and the model line of ~60 m/s, i.e. the model spectrum is expected to be about 60 m/s narrower than the one of Gl 273. Convective velocities have not yet been observed in M-dwarfs, but they are not expected to change significantly within the early- and mid-M stars either[3]. Thus, there is no reason to believe that the intrinsic spectrum of Gl 273 (i.e., the spectrum of an early M star with no rotation) is smaller than the modeled spectral line.

The convolution of the instrumental profile and the synthetic Fe I line is overplotted over the data in Fig. 3 (red line). The Fe I line was scaled using an optical depth scaling to account for saturation (the scaling factor was approximately unity). It is immediately clear that our expectation of an observed Fe I line has a shape that very accurately matches the line shape observed in the two FeH lines in question.

What does the consistency of synthetic Fe I lines and the FeH lines mean in terms of rotational broadening? The intrinsic line broadening in Fe and FeH lines can be expected to be similar since the main broadening mechanisms are comparable; in particular there is no reason to assume that the FeH lines in Gl 273 should be *narrower* than the Fe I lines at the atmospheric parameters used in the model. That means that no indication for extra broadening due to rotation is found in the observed lines. The similarity of the two FeH lines in Gl 273 to the shape expected for observed Fe lines means that within the uncertainties the FeH lines are consistent with zero rotation.

[3] The vanishing of a radiative core does not significantly affect the photospheric velocities.

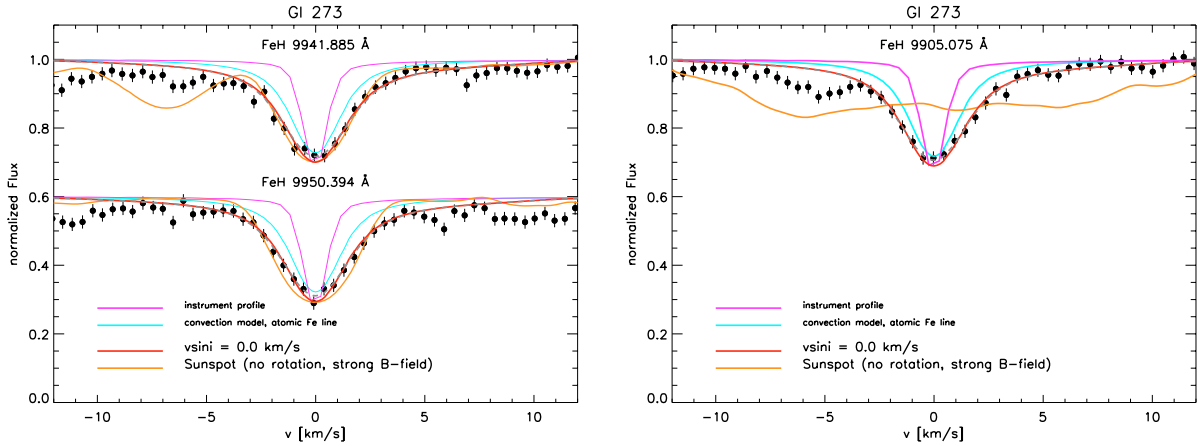

Fig. 3. Spectral lines of Gl 273. Overplotted are the instrumental profile (magenta), a model of an Fe I line (cyan), the convolution of instrumental and model profiles (red), and a sunspot spectrum of the same region (orange). *Left*: the two magnetically insensitive lines; *right*: a magnetically sensitive line, note the strong Zeeman broadening in the sunspot spectrum.

3.2. Zeeman sensitivity of the spectral lines

In Fig. 3, a spectrum of a sunspot[4] is plotted over the data (orange). This spectrum is formed in a somewhat hotter environment than the M dwarf spectrum and in a strong magnetic field (∼2 kG), but it is not rotationally broadened since the spot is spatially resolved. The two lines shown in the left panel resemble the two lines in the spectral region that are least affected by Zeeman broadening consistent with the analysis of the FeH band observed at lower resolution in Reiners & Basri (2006). In the first line (λ9942 Å), the sunspot spectrum resembles the M-dwarf spectrum very accurately, it is a little broader in the core (probably due to the larger temperature broadening) and an extra component shows up at $-7\,\mathrm{km\,s^{-1}}$. Again, there is no indication for rotational broadening in the integrated spectrum of Gl 273 from comparing its FeH lines to the sunspot spectrum. The second line (λ9950 Å) appears somewhat broader in the sunspot spectrum. This cannot be ascribed to convection since it is not seen in the λ9942 Å line (where the sunspot line matches the M dwarf line), hence the extra broadening in the FeH line at 9942 Å must be due to the strong magnetic field of the sunspot. The strong effect of Zeeman broadening on a magnetically sensitive FeH line is shown in the right column of Fig. 3, in which the same as in the left panel is shown but for the line at $\lambda = 9905$ Å. This line is very sensitive to magnetic fields, which can be seen in the heavy broadening of the sunspot spectrum. This comparison also shows that Zeeman broadening is extremely small in the two lines of the left panel. Thus, for the analysis of rotational broadening, we can minimize the effect of Zeeman broadening employing only the two magnetically insensitive lines (left panel in Fig. 3). As a byproduct, it becomes clear that Gl 273 can only have a very weak mean magnetic field (that the product of magnetic field and surface coverage is very small).

In this paper I will not determine the magnetic fluxes of the observed targets. Reiners & Basri (2006) show a method to measure the magnetic flux interpolating between the spectrum of a star with strong flux and a star with weak or zero flux. With the CES data, a more accurate analysis of the strength and of the pattern of Zeeman broadening in lines of the FeH molecule is possible but goes beyond the scope of this paper.

[4] Available at `ftp://ftp.noao.edu/fts/spot3atl`

3.3. Detection threshold

To estimate the lowest rotation velocity that can be detected in our data, the comparison spectrum, i.e. the Fe I line broadened according to the instrument resolution, was artificially spun up to a $v \sin i$ of $1\,\mathrm{km\,s^{-1}}$. The result is overplotted in Fig. 3 as dashed lines, but it essentially remains hidden below the curve for $v \sin i = 0\,\mathrm{km\,s^{-1}}$. Such small a rotation broadening is difficult to see even in the high quality data used here. It is important to realize that a rotation velocity of $v \sin i = 1\,\mathrm{km\,s^{-1}}$ is hardly detectable at a resolution of $R = 200\,000$ in an M-star, which has a very narrow intrinsic line shape due to the small temperature broadening. At lower resolving power this threshold grows, and small rotation becomes more difficult to detect.

The comparison shows that a projected rotation velocity of $v \sin i = 1\,\mathrm{km\,s^{-1}}$ cannot be ruled out for Gl 273. At higher velocities, however, a difference of $1\,\mathrm{km\,s^{-1}}$ is rather easy to detect (compare to the case of Gl 229A in the right panel of Fig. 4) as soon as rotational broadening becomes a significant fraction of the intrinsic width. Thus, from visual comparison, the detection threshold for rotation broadening in data of this quality is estimated to $\Delta v \sin i = 1\,\mathrm{km\,s^{-1}}$, and $v \sin i \leq 1\,\mathrm{km\,s^{-1}}$ is adopted for Gl 273.

3.4. Significant rotation

All other sample stars show FeH lines significantly broader than the lines in Gl 273. Since both lines are not sensitive to Zeeman broadening, the extra broadening must be due to rotation or differences in convective motion. The latter is probably very small in the narrow range of spectral types (Gl 273 has a spectral type of M 3.5), and I will assume that rotation is the only extra broadening mechanism for what follows. To determine the value of $v \sin i$, the template spectrum (see below) is artificially broadened searching for the best match to the data in both lines. The best fit was determined by eye, which is sufficient to the level of accuracy achieved here (see below). In all cases, the two FeH lines yielded consistent results.

The template lines were constructed using a combination of the artificial spectrum of the Fe I line and the observed lines from Gl 273. In order to minimize the effects of limited *SNR* in the spectrum of Gl 273, that spectrum was smoothed using a 3 pixel box-car. The smoothed spectrum was only used in the wings of the template spectrum. In the core of the lines, such an

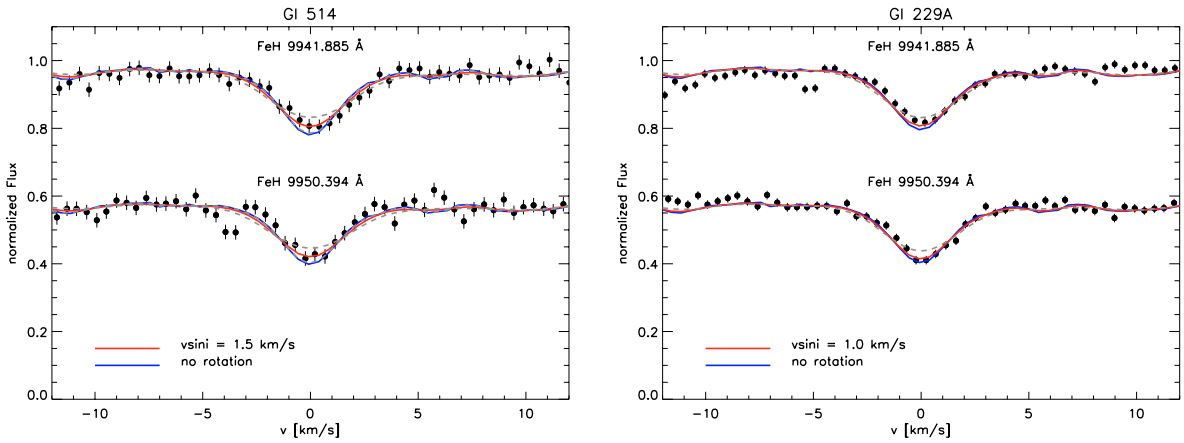

Fig. 4. The two magnetically insensitive spectral lines of Gl 514 (*left*) and Gl 229A (*right*). The template profile (see text) is overplotted in blue, the red line shows the best fit with rotational broadening given in the plot. Dashed lines show artificial broadening for $v \sin i \pm 1\,\mathrm{km\,s^{-1}}$.

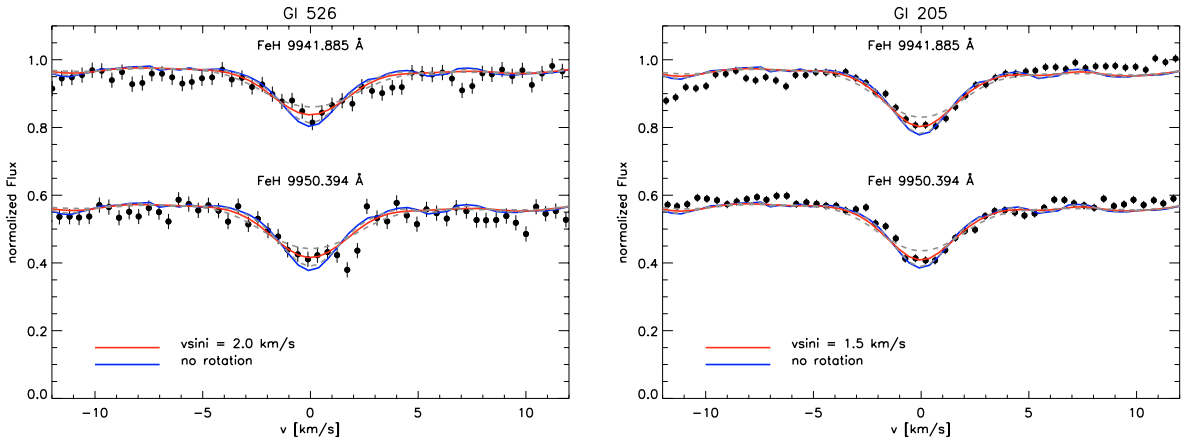

Fig. 5. Same as Fig. 4 but for Gl 526 (*left*) and Gl 205 (*right*).

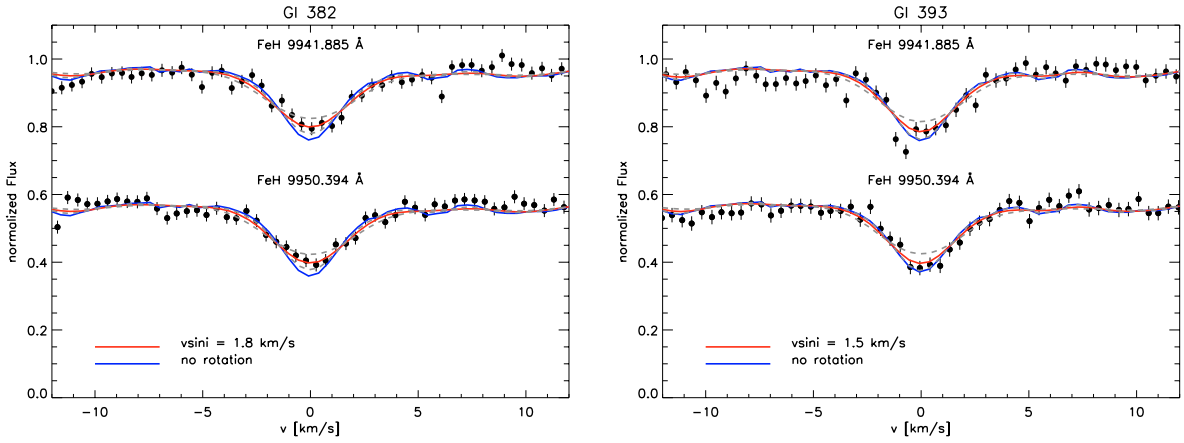

Fig. 6. Same as Fig. 4 but for Gl 382 (*left*) and Gl 393 (*right*).

approach would lead to an effective broadening of the line mimicking higher rotation velocity. On the other hand, the artificial spectrum of the broadened Fe I line accurately resembles the line core of the two lines, and it was used instead of the original data spectrum in the core region between $\pm 3\,\mathrm{km\,s^{-1}}$.

The template spectrum was scaled and artificially broadened to match the spectra of the sample targets. Figures 4–8 show the two FeH lines for all stars together with the best fits. For comparison, two artificial spectra at $v \sin i = v \sin i_{\rm fit} \pm 1\,\mathrm{km\,s^{-1}}$ are also plotted (dashed lines) demonstrating the sensitivity in $v \sin i$. It can be seen that the data quality allows to determine the value of $v \sin i$ within an uncertainty of $\pm 1\,\mathrm{km\,s^{-1}}$.

3.5. Rotation velocities from cross-correlation

A very successful method used to measure stellar rotation velocities in stars and brown dwarfs of spectral types M and L is the cross correlation method (e.g., Basri et al. 2000; Mohanty & Basri 2003; Bailer-Jones 2004). A spectrum of a slowly rotating star is used as a template, it is artificially broadened and

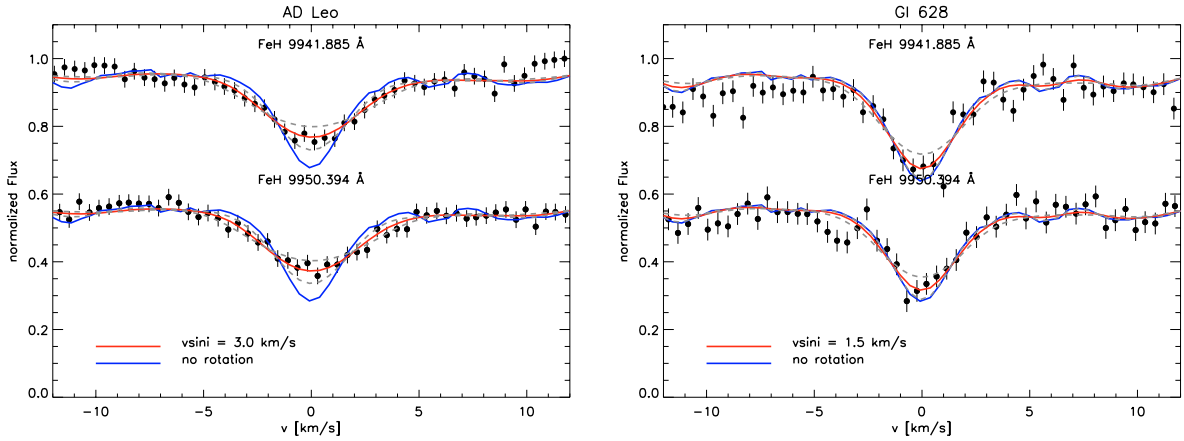

Fig. 7. Same as Fig. 4 but for AD Leo (*left*) and Gl 628 (*right*).

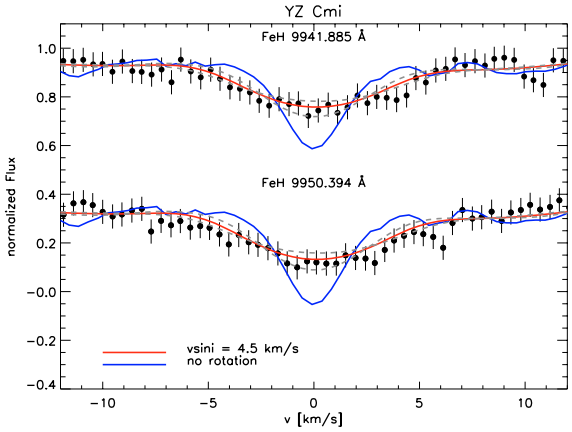

Fig. 8. Same as Fig. 4 but for YZ Cmi.

the width of the cross-correlation function between the unbroadened template and its broadened version is calibrated for various rotation speeds. Then, the cross-correlation between a star and the template is calculated and the width of this profile is compared to the set of calibrations obtained before. One caveat of this method is that it cannot account for Zeeman broadening. Effectively, an average of the rotation broadening from all lines is calculated. Hence it could be argued that for the magnetically active stars the cross-correlation method yields systematically too high values for $v \sin i$. This hypothesis can be tested by comparing results from cross-correlation to results from direct line fitting of magnetically insensitive lines.

I calculated the cross-correlation functions for the sample stars in the full wavelength range of the observations using the slowest rotator in the sample, Gl 273, as a template. A second set of $v \sin i$ values is calculated this way, the results are given in the fourth column of Table 2. It is immediately clear that in the domain of very slow rotation, $v \sin i \lesssim 5\,\mathrm{km\,s^{-1}}$, the result from line fitting and cross-correlation agree very well, less (if any) influence can be expected at higher rotation. It appears that magnetic broadening does not influence the measurement of rotation via the cross-correlation method in this spectral region. The difference in spectral type does not appear to influence this result. It is important to note that this spectral region is dominated by absorption from FeH lines, and that the structure of this band does not significantly change in the spectral range investigated. In a region with different absorbing species (and larger spectral coverage) larger differences can be expected.

4. Results

4.1. Rotation of the sample stars

In all stars but one, significant rotational line broadening is detected. Only the spectral lines of Gl 273 do not show any broadening in excess of what is expected from the Fe I model and the instrumental profile. The spectral lines of Gl 273 are also significantly narrower than the lines in all other stars. The uncertainty and the detection threshold for the projected rotation velocity $v \sin i$ is $\sim$1 km s^{-1} (see above).

The measured values of $v \sin i$ are given in Table 2 together with literature values from former publications. In all but one cases, this work yields rotation velocities lower than what was previously reported. In six stars, literature contained only upper limits of about 3 km s^{-1} for $v \sin i$, and this work provides detection of rotation of or below 2.0 km s^{-1} for five of them. In Gl 273, Delfosse et al. (1998) report an upper limit of $v \sin i \leq 2.4\,\mathrm{km\,s^{-1}}$ (although this accuracy seems a little optimistic given the resolution of their data). The upper limit on the projected rotation velocity of Gl 273 is now as low as $v \sin i \leq 1.0\,\mathrm{km\,s^{-1}}$. In three stars, a detection of rotation was reported before, the three cases are the following:

1. Gl 229A ($v \sin i = 1.0\,\mathrm{km\,s^{-1}}$): Vogt et al. (1983) report $v \sin i = 3.0\,\mathrm{km\,s^{-1}}$, but in their table of results they indicate that this value is uncertain. They used a Ba II line at $\lambda = 6141$ Å at a resolution of $R = 50\,000$ (FWHM of $6\,\mathrm{km\,s^{-1}}$). Such low a rotation velocity has a very subtle effect in a single line and their result may be interpreted as an upper limit as well.
2. AD Leo ($v \sin i = 3.0\,\mathrm{km\,s^{-1}}$): this famous flare star has been a frequent subject to rotation measurements. Vogt et al. (1983); Marcy & Chen (1992); Delfosse et al. (1998); Fuhrmeister et al. (2004) all measure $v \sin i$ between 5 and 7.6 km s^{-1} from either fits to single atomic lines (Vogt et al. 1983; Marcy & Chen 1992), the cross correlation method (Delfosse et al. 1998), or fitting large parts of the spectrum (Fuhrmeister et al. 2004). However, they all use wavelength regions that do not contain isolated lines but either single lines embedded in a continuum affected by molecular absorption, or molecular bands that consist of many blended features. The resolution of the data they use is also a factor of 2–4 lower than what was available here. Apparently, the higher data quality and in particular the use of isolated features allows the detection of the low rotation velocity in AD Leo while slow rotation is hidden in lower resolution

Table 2. Results.

Name	$B-V^a$	$v \sin i$ km s^{-1}	$v \sin i_{\rm Xcorr}$ km s^{-1}	$v \sin i_{\rm Lit}$ km s^{-1}	R^b $R_\odot$	$\frac{P}{\sin i}$ d	$L^c_{\rm bol}$ erg s^{-1}	$L^d_{\rm X}$ erg s^{-1}	$\log(\frac{L_{\rm X}}{L_{\rm bol}})$	$\log Ro$
Gl 514	1.49	1.5	1.3	<2.9^e	0.60	20.3	32.11	27.38	–4.73	–0.11
Gl 229A	1.50	1.0	1.0	3.0^f	0.69	35.0	32.27	27.11	–5.16	0.11
Gl 526	1.43	2.0	1.4	<2.9^e	0.50	12.7	32.12	26.87	–5.25	–0.32
Gl 205	1.47	1.5	1.0	<2.9^e	0.79	26.8	32.39	27.66	–4.73	0.00
Gl 382	1.50	1.8	1.3	<2.9^e	0.69	19.4	32.26	27.45	–4.81	–0.14
Gl 393	1.51	1.5	1.1	<2.9^e	0.52	17.7	32.02	26.98	–5.04	–0.19
Gl 273	1.57	≤1.0	0.0^g	< 2.4^e	0.35	>17.9	31.64	26.03	–5.61	–0.19
AD Leo	1.53	3.0	3.0	6.2^e	0.50	8.4	31.94	28.58	–3.36	–0.51
Gl 628	1.58	1.5	1.1	<1.1^e	0.32	10.7	31.60	26.79	–4.81	–0.42
YZ CMi	1.61	4.5	5.3	6.5^e	0.30	3.4	31.68	28.57	–3.11	–0.92

[a]Leggett (1992). [b]Lacy (1977). [c] Using calibration from Delfosse et al. (1998), $M_{\rm V}$ from Gliese & Jahreiss (1991) and $R-I$ from Leggett (1992). [d] From NEXXUS database (Schmitt & Liefke 2004), i.e. ROSAT data. [e] Delfosse et al. (1998). [f] Vogt et al. (1983). [g] Used as template for Cross Correlation.

data in broad parts of the spectrum. Reiners & Basri (2007) also determine $v \sin i \approx 3\,{\rm km\,s^{-1}}$ from data in the same wavelength region at lower spectral resolution and explicitly taking into account Zeeman broadening. Whether effects of magnetic fields mimic more rapid rotation at other wavelength regions, is difficult to assess. AD Leo is a flare star and Reiners & Basri (2007) measure a net magnetic flux of $Bf \sim 3\,{\rm kG}$, thus significant broadening may affect the spectral features in large parts of the spectrum. However, Marcy & Chen (1992) addressed this question finding that the lines they used are not affected by Zeeman broadening, and the results from cross-correlation analysis in Sect. 3.5 show that Zeeman broadening does not lead to a systematic offset in the measurements of $v \sin i$ even in a wavelength region that contains absorption features with rather strong Zeeman sensitivity.

3. YZ Cmi ($v \sin i = 4.5\,{\rm km\,s^{-1}}$): Delfosse et al. (1998) and Fuhrmeister et al. (2004) find a value of $v \sin i$ of $6.5\,{\rm km\,s^{-1}}$ instead of the $4.5\,{\rm km\,s^{-1}}$ reported here. Marcy & Chen (1992) find $v \sin i = 4.8\,{\rm km\,s^{-1}}$ but admit poor data quality. YZ CMi is also a flare star with an even stronger magnetic flux ($Bf \sim 4\,{\rm kG}$ according to Reiners & Basri 2007), hence the case of YZ Cmi may be similar to AD Leo. However, the difference of $2\,{\rm km\,s^{-1}}$ may not be considered significant, and the new (lower) value comes from significantly better data.

4.2. The rotation-activity connection in very slowly rotating M-stars

The ratio of X-ray to bolometric luminosity is a good indicator of stellar magnetic activity. For all sample stars, X-ray luminosity is available in the NEXXUS database (i.e., ROSAT data, Schmitt & Liefke 2004). Bolometric luminosity is calculated using the calibration in Delfosse et al. (1998) with $M_{\rm V}$ from Gliese & Jahreiss (1991) and $R-I$ color from Leggett (1992). The ratio of X-ray to bolometric luminosity for the stars of this sample is plotted versus $v \sin i$ in the left panel of Fig. 9, and versus the Rossby number (the ratio of Period to convective overturn time) in Fig. 10.

It should be noted that X-ray luminosities from the ROSAT measurements have very high internal precision, but there is some debate about the conversion factor between the count rate and the flux. Schmitt et al. (1995) also reports X-ray luminosities for stars in the solar neighborhood from ROSAT data using mostly the same data but a slightly different conversion factor than the one in Schmitt & Liefke (2004). Although the differences between the two calibrations are sometimes significant, they do not change the interpretation of the sample used here. The same is true for intrinsic variability of X-ray luminosities, which in the active M dwarfs can be on the order of a few tenths of a dex (e.g., Robrade & Schmitt 2005).

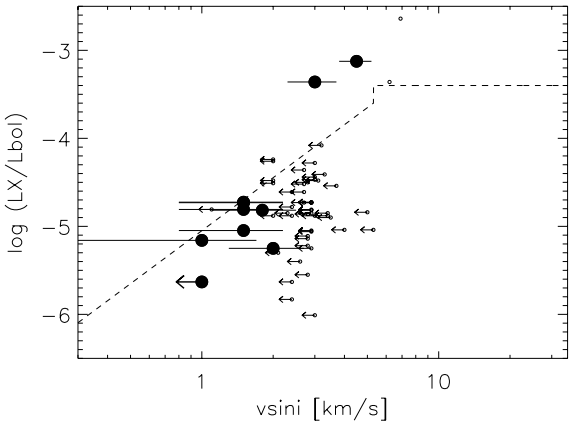

Fig. 9. $\log L_{\rm X}/L_{\rm bol}$ vs. $v \sin i$ for early M-dwarfs (including YZ Cmi, M4.5). New rotation measurements are plotted as full circles, data from Delfosse et al. (1998) as small open circles (most of their $v \sin i$ values are upper limits). $\log L_{\rm X}/L_{\rm bol}$ for the stars of this sample were recalculated as explained in the text.

4.2.1. Activity and projected rotation velocity

The sample used here consists of two groups; I) stars with high X-ray to bolometric luminosity ratio ($\log L_{\rm X}/L_{\rm bol} > -3.5$) and II) stars with a low ratio of $\log L_{\rm X}/L_{\rm bol} < -4.5$. All stars in group II) have values of $v \sin i \le 2\,{\rm km\,s^{-1}}$ while the two stars in group I) (AD Leo and YZ Cmi) are more rapid rotators. The two groups of stars are clearly separated in the $L_{\rm X}/L_{\rm bol}$ vs. $v \sin i$ plot (Fig. 9). The most obvious result from this work is that the bulk of the very inactive stars (group II) indeed has rotation velocities significantly lower than $v \sin i = 3\,{\rm km\,s^{-1}}$.

Among the low-activity group, projected rotation velocities between 1 and $2\,{\rm km\,s^{-1}}$ are measured. The detected (projected) rotation velocities are consistent with a rotation-activity connection in the sense that most stars at $v \sin i \sim 2\,{\rm km\,s^{-1}}$ have higher $\log L_{\rm X}/L_{\rm bol}$ than the slowest rotators at $v \sin i \sim 1\,{\rm km\,s^{-1}}$. Seven of the eight objects (among the low-activity subsample)

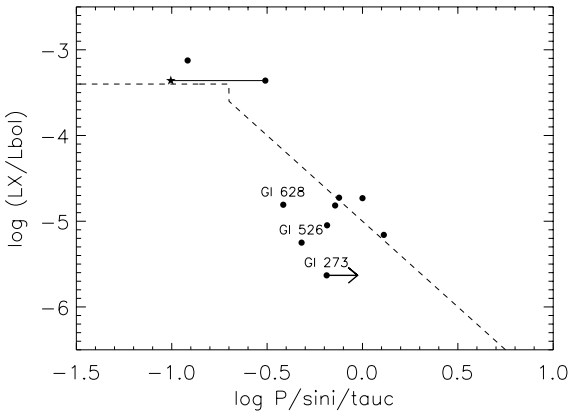

Fig. 10. Normalized X-ray luminosity against Rossby number for the sample. AD Leo is plotted at two different Rossby numbers, the filled circle is the value from $v \sin i$ measurements, the star is from the period given by Spiesman & Hawley (1986).

follow a rather tight trend that falls only slightly below the relation expected from an extrapolation of the rotation-activity connection found in hotter stars (dashed line in Fig. 9; note that Gl 205 and Gl 514 share the same point). The only star that is a little off the track is Gl 526, which has the highest rotation velocity ($v \sin i = 2.0\,\mathrm{km\,s^{-1}}$) among the low-activity subsample, but even among them shows comparably low activity ($\log L_\mathrm{X}/L_\mathrm{bol} < -5$).

It has to be taken into account that it is only the *projected* rotation velocity that is measured here, so that the true rotation speed indeed is higher than $v \sin i$. Statistically, every measurement is underestimated by a factor of $\pi/4$, but that does not help intercomparing rotation velocities in a sample. The projection may move the measured rotation velocities of individual stars further to the right in Fig. 9, however, it cannot be expected that this has significant influence on the trend among the seven stars mentioned. Correcting for the projection effect in a statistical sense does indeed move the stars further away from the dashed line, but as was mentioned earlier, the absolute position of this line is not a crucial point.

Considering Gl 526 as an outlier, seven objects define a very close rotation-activity connection in the early M-dwarfs rotating slower than 3 $\mathrm{km\,s^{-1}}$. Gl 526 has a spectral type of M 1.5 and there is no reason to believe that there is any difference to the other seven slow rotators. A small inclination angle would mean that Gl 526 is indeed rotating even more rapidly, so a projection effect would make the inconsistency worse. However, the intrinsic scatter among hotter stars in the rotation-activity relation is often much stronger than the difference between Gl 526 and the other stars of the sample.

The two sample stars with a much higher ratio of X-ray to bolometric luminosity in the sample, AD Leo and YZ Cmi, are consistent with the rotation-activity connection in the sense that they are more active while rotating more rapidly than the inactive stars of the sample. However, the relatively large difference of more than one order of magnitude in $L_\mathrm{X}/L_\mathrm{bol}$ is only accompanied by a difference of 1–2 $\mathrm{km\,s^{-1}}$ in $v \sin i$ between AD Leo and the slower rotators. This would be a rather abrupt change in activity or a very steep rise in the rotation-activity connection at velocities around 3 $\mathrm{km\,s^{-1}}$. Spiesman & Hawley (1986) report a rotation period of AD Leo of 2.7 d which would indicate a higher rotation velocity around $v \approx 10\,\mathrm{km\,s^{-1}}$ observed under a rather low inclination angle (see Sect. 4.2.2).

At high rotation, there is no doubt that among early M-stars activity saturates rather early (at comparably low rotation rates) while very slow rotators ($v \sin i \lesssim 2\,\mathrm{km\,s^{-1}}$) have very low activity ($\log L_\mathrm{X}/L_\mathrm{bol} \lesssim -4.5$). The gap between the "very slow" rotators and the saturation regime could not be bridged with this sample, and observations of stars probing activity around $\log L_\mathrm{X}/L_\mathrm{bol} \approx -4$ are required.

4.2.2. Activity and Rossby number

So far the rotation-activity connection was only investigated in terms of surface velocity. A parameter that seems to play a more important role at least in solar-type stars is the Rossby number, that is the ratio of the rotation period P to the convective overturn time τ_c (Noyes et al. 1984). The ratio of X-ray to bolometric luminosity is plotted against the Rossby number (Ro) in Fig. 10. To calculate Ro for the sample object, the period was derived using the projected rotation velocity and the radii given in Lacy (1977). Thus, only the projected rotation period $P/\sin i$ is available. Convective overturn times for the sample stars were calculated from Eq. (4) in Noyes et al. (1984). Other calculations of Gilliland (1986) and more recently Kim & Demarque (1996) differ only little from the results of Noyes et al. (1984). Since the spectral types of the sample are all very similar, using other versions of τ_c changes the results very little (in fact, it would shift all points *and* the relation expected from hotter stars towards lower Rossby numbers).

The individual values of τ_conv used for the calculation of Ro may be questioned. Nevertheless, there is a clear indication that the field M-dwarfs in Fig. 10 generally follow the same rotation-activity relation as hotter and younger stars. Stars with the smallest Rossby numbers show saturated emission of $\log L_\mathrm{X}/L_\mathrm{bol} \approx -3$, those with higher Rossby number are less active. The scatter in Rossby number among the inactive stars at given $L_\mathrm{X}/L_\mathrm{bol}$ is about half a dex, which is not larger than the scatter in samples of hotter stars on the non-saturated part of the rotation-activity connection (e.g. Patten & Simon 1996). AD Leo may have a somewhat high (projected) Rossby number for its high activity. This may be due to a small inclination angle as mentioned above. The position of AD Leo shifts significantly to the left if the suggested period of 2.7 d (Spiesman & Hawley 1986) is used, it is indicated with a star instead of a circle in Fig. 10. However, the presence of a rotation period of 2.7 d of AD Leo in the data of Spiesman & Hawley (1986) may be debatable, Torres et al. (1982) also report a period of 2.6 d but they also put a question mark to their result. On the other hand, regardless of what the rotation period of AD Leo really is, even the longest possible period of 8.4 d taken from the new value of $v \sin i$ would lead to a Rossby number smaller than the ones in the inactive stars.

Finally, the Rossby number at which activity becomes saturated is consistent with the rotation-activity relation in hotter stars. Patten & Simon (1996) show that the transition from the active stars to inactive stars occurs rather rapidly around a value of $Ro \approx 0.3$ ($\log Ro \approx -0.5$), just where it occurs in Fig. 10, as well.

5. Summary

This study probes the validity of the rotation-activity connection – i.e. stars show saturated activity at low Rossby numbers and decreasing activity as Rossby number grows larger than ∼0.3 – in stars with very deep convection zones near the boundary to fully convective stars. These early M-stars have very long convective overturn times, so that stars populating the non-saturated

part of the rotation-activity connection need to be very slow rotators with rotation periods of several weeks or equatorial rotation velocities lower than $\sim 3\,\mathrm{km\,s^{-1}}$. Accurate rotation velocities were measured in eight probably not fully convective stars with low activity ($\log L_\mathrm{X}/L_\mathrm{bol} < -4.5$) for which only upper limits in $v \sin i$ were available (for Gl 229A, a detection of $v \sin i = 3\,\mathrm{km\,s^{-1}}$ was reported earlier, but here $v \sin i = 1\,\mathrm{km\,s^{-1}}$ is measured). All eight inactive stars show projected rotation velocities of or below $v \sin i = 2\,\mathrm{km\,s^{-1}}$.

For the first time, narrow absorption lines of molecular FeH were intrinsically resolved. Comparison to a model of an atomic Fe I absorption line shows that the line shape of that model is qualitatively consistent with the observations. This allows a deeper investigation of M-star convective patterns in high quality data in this spectral range.

The main conclusion of this study is that the rotation activity connection that is valid in stars of spectral types F–M among rapidly rotating cluster stars, and stars of spectral type F–K in the field (Noyes et al. 1984; Patten & Simon 1996; Pizzolato et al. 2003), is still valid in the early field M-dwarfs after they have spun down to very low rotation rates. Thus, the rotation activity connection holds in all main-sequence field stars that harbor a convective envelope.

Acknowledgements. The author thanks Thomas Dall, who was the instrument scientist at the time of observation, for professional and very enjoyable support, and S. Wedemeyer and H.-G. Ludwig for providing the Fe line profile. A.R. has received research funding from the European Commission's Sixth Framework Programme as an Outgoing International Fellow (MOIF-CT-2004-002544).

References

Bailer-Jones, C. A. L. 2004, A&A, 419, 703
Barbera, M., Micela, G., Sciortino, S., Harnden, Jr., F. R., & Rosner, R. 1993, ApJ, 414, 846
Basri, G. 1986, Proceedings of the Fourth Cambridge Workshop on Cool Stars, Stellar Systems, and the Sun, Lecture Notes in Physics, ed. M. Zeilik, & D. M. Gibson, (Springer-Verlag), 254, 184
Basri, G., Mohanty, S., Allard, F., et al. 2000, ApJ, 538, 337
Benedict, G. F., McArthur, B., Nelan, E., et al. 1998, AJ, 116, 429
Bessel, M. S. 1990, A&AS, 83,357
Delfosse, X., Forveille, T., Perrier, C., & Mayor, M. 1998, A&A, 331, 581
Durney, B. R., & Latour, J. 1978, Geophys. Ap. Fluid. Dyn., 9, 241
Fleming, T. A., Giampapa, M. S., Schmitt, J. H. M. M., & Bookbinder, J. A. 1993, ApJ, 410, 387
Fleming, T. A., Giampapa, M. S., & Schmitt, J. H. M. M. 2000, ApJ, 533, 372
Fuhrmeister, B., Schmitt, J. H. M. M., & Wichmann, R. 2004, A&A, 417, 701
Giampapa, M. S., Rosner, R., Kasyap, V., et al. 1996, ApJ, 463, 707
Gilliland, R. L. 1986, ApJ, 300, 399
Gizis, J. E., Reid, I. N., & Hawley, S. L. 2002, AJ, 123, 3356
Gliese, W., & Jahreiss, H. 1991, Third Catalogue of Nearby Stars (Heidelberg: Astron. Rechen Inst.)
Haisch, B. M., Butler, C. J., Foing, B., Rodonó, M., & Giampapa, M. S. 1990, A&A, 232, 387
Hawley, S. L., Gizis, J. E., & Reid, I. N. 1996, AJ, 112, 2799
Herbst, W., & Miller, J. R. 1989, AJ, 97, 891
Kim, Y.-C., & Demarque, P. 1996, ApJ, 457, 340
Lacy, C. H. 1977, ApJS, 34, 479
Leggett, S. K. 1992, ApJS, 82, 351
López-Morales, M. 2007, [arXiv:astroph/0701702]
Macry, G. W., & Chen, G. H. 1992, ApJ, 390, 550
Mohanty, S., & Basri, G. 2003, ApJ, 583, 451
Mohanty, S., Basri, G., Shu, F., Allacr, F., & Chabrier, G. 2002, ApJ, 571, 469
Noyes, R. W., Hartmann, L. W., Baliunas, S. L., Duncan, D. K., Vaughan, A. H. 1984, ApJ, 279, 763
Patten, B. M., & Simon, T. 1996, ApJS, 106, 489
Parker, E. N., ApJ, 163, 279
Pettersen, B. R. 1982, Activity in Red-Dwarf Stars, IAU Coll. 71, ed. P. B. Byrne, & M. Rodono, ASSL, 102
Pettersen, B. R., Lambert, D. L., Tomkin, J., Sandmann, W. H., & Lin, H. 1987, A&A, 183, 66
Pizzolato, N., Maggio, A., Micela, G., Sciortino, S., & Ventura, P. 2003, A&A, 397, 147
Randich, S., Schmit, J. H. M. M., Prosser, C. F., & Stauffer, J. R. 1996, A&A, 305, 785
Reid, I. N., Kirkpatrick, J. D., Gizis, J. E., & Liebert, J. 1999, ApJ, 527, 105
Reid, I. N., Hawley, S. L., & Gizis, J. E. 1995, AJ, 110, 1338
Reiners, A., & Basri, G. 2006, ApJ, 644, 509
Reiners, A., & Basri, G. 2007, ApJ, 656, 1121
Robrade, J., & Schmitt, J. H. M. M. 2005, A&A, 435, 1073
Schmitt, J. H. M. M., & Liefke, C. 2004, A&A, 417, 651
Schmitt, J. H. M. M., Fleming, T. A., & Giampapa, M. S. 1995, ApJ, 450, 392
Singh, K. P., Drake, S. A., Gotthelf, E. V., & White, N. E. 1999, ApJ, 512, 874
Spiesman, W. J., Hawley, S. L. 1986, AJ, 92, 664
Torres, C. A. O., Busko, I. C., & Quast, G. R. 1982, Activity in Red-Dwarf Stars, ed. P. B. Byrne, & M. Rodono, ASSL, 102, IAU Coll. 71
Vogt, S. S., Soderblom, D. R., & Penrod, G. D. 1983, ApJ, 269, 250
Wedemeyer, S., & Ludwig, H.-G. 2006, priv. comm.
West, A. A., Hawley, L., Walkouvicz, L. M., et al. 2004, AJ, 128, 426